Journal of Engineering Physics and Thermophysics, Vol. 76, No. 3, 2003

EXACT SOLUTION OF THE PROBLEM OF FLOW OF A POLYMER SOLUTION IN A PLANE CHANNEL

S. N. Aristov and O. I. Skul'skii

UDC 532.135

One-dimensional flow of polymer solutions in a plane channel under the action of the pressure gradient has been considered. To describe the rheological properties of the solutions we have selected: 1) generalization of the Jeffreys phenomenological model with an objective time derivative F_{abc} with six arbitrary material constants; 2) the differential vector model proposed by Remmelgas, Harrison, and Leal and that is the approximation of the Doi–Edwards–Marrucci–Grizzuti model. Exact analytical solutions of the problem of flow in a plane channel have been obtained for them. In the two cases the problem can have both a unique solution and a nonunique solution. The velocity profiles are either smooth nearly parabolic or have weak tangential discontinuities. Criterial conditions for the appearance of ambiguous flow regimes have been obtained.

Despite lengthy investigations, problems of modeling and stability of viscoelastic-liquid flows remain topical in the rheology and technology of processing of polymer materials. Study of the reasons for the appearance of the so-called spurt effects, i.e., disturbances in the stability of liquid flow out of capillaries and channels, has attracted the particular attention of researchers [1–5]. Mathematical modeling of them involves investigation of the existence, uniqueness, and stability of solutions to the equations of motion of viscoelastic liquids.

Numerous rheological models exist at present which allow for elasticity effects in the case of flow of polymer solutions and melts. This work seeks to investigate the effectiveness of two models obtained by different methods with the example of plane-parallel channel flow under the action of a prescribed gradient rather than to describe the behavior of a certain specific material.

Consideration has been primarily given to the Jeffreys phenomenological model of a viscoelastic liquid with an objective time derivative F_{abc} with arbitrary material constants a, b, and c (model A). This version of a rheological model is a particular case of the Oldroyd eight-constant model in which the time derivatives for extra stresses and deformation rate contain identical material constants. At the same time, the models of Maxwell, De Witt, and White and Metzner and the three- and four-constant models of Oldroyd can be considered as particular cases of the generalized six-constant model of Jeffreys.

The second of the selected models has been obtained on the basis of statistical description of the orientation and elongation of coiled macromolecules with subsequent averaging to a macrolevel. This model is based on the reptile concept introduced by De Gennes and elaborated further by Doi and Edwards. In the Doi–Edwards (DE) model, each polymeric molecule was considered as a flexible nonelongating chain moving in the tube formed by other molecules [6]. In more recent times, owing to the investigations of Pearson, Leal, Marrucci and Grizzuti, the Doi–Edwards model was modified to allow for the orientation and elongation of each segment of a polymer chain [7]. The resulting DEMG model most adequately describes the dynamics of macromolecules but it is very cumbersome for numerical calculations of actual flows. To approximate the DEMG model Remmelgas, Harrison, and Leal have developed the differential vector model (RHL) with the nonlinear parameter of elasticity of a coiled macromolecule for description of the effect of internal cross-links [8, 9]. It has been assumed that the orientational relaxation time τ_d is much longer than the relaxation time of elongation τ_R. Owing to such an assumption, one can consider the orientation and the elongation of a chain separately by introducing the vector $\mathbf{R} = R\mathbf{u}$. In our work, we consider a simplified variant of the RHL model with a linear elasticity parameter (model B).

Institute of Continuum Mechanics, Ural Branch of the Russian Academy of Sciences, Perm', Russia; email: skul@icmm.ru. Translated from Inzhenerno-Fizicheskii Zhurnal, Vol. 76, No. 3, pp. 88–95, May–June, 2003. Original article submitted September 6, 2002.

1062-0125/03/7603-0577$25.00

The present investigation seeks to compare the analytical solutions of the equations of motion for the two selected models under the assumption of the one-dimensional flow in a plane channel and to separate kinematically feasible and physically realizable ones out of them on the basis of the existing results of stability theory.

1. Formulation of the Boundary-Value Problem. Let us consider the formulation of the problem of viscoelastic-liquid flow in a plane channel under the action of the pressure gradient. The equation of motion in terms of extra stresses has the form

$$\rho\left[\frac{\partial \mathbf{v}}{\partial t} + \mathbf{v}\cdot\nabla\mathbf{v}\right] = -\nabla p + \nabla\cdot\tau\,.$$

The liquid will be considered to be incompressible:

$$\nabla\cdot\mathbf{v} = 0\,.$$

The equations of motion must be supplemented with governing relations and corresponding boundary conditions.

Model A. The Jeffreys equation with the most general associated time derivative which preserves symmetry has the form $\tau + \lambda_1 F_{abc}\tau = \mu(\mathbf{D} + \lambda_2 F_{abc}\mathbf{D})$ or in expanded form it is

$$\boldsymbol{\tau} + \lambda_1\left[\frac{D\boldsymbol{\tau}}{Dt} - \mathbf{W}\cdot\boldsymbol{\tau} + \boldsymbol{\tau}\cdot\mathbf{W} + a\,(\boldsymbol{\tau}\cdot\mathbf{D} + \mathbf{D}\cdot\boldsymbol{\tau}) + b\,(\boldsymbol{\tau}:\mathbf{D})\,\mathbf{I} + c\mathbf{D}\,\mathrm{tr}\,(\boldsymbol{\tau})\right] =$$

$$= 2\mu\left[\mathbf{D} + \lambda_2\left(\frac{D\mathbf{D}}{Dt} - \mathbf{W}\cdot\mathbf{D} + \mathbf{D}\cdot\mathbf{W} + 2a\,(\mathbf{D}\cdot\mathbf{D}) + b\,(\mathbf{D}:\mathbf{D})\,\mathbf{I}\right)\right].$$

Model B. The governing equation for the polymer solution is written with account for the representation of the vector $\mathbf{R} = R\mathbf{u}$:

$$\boldsymbol{\tau} = 2\eta_s\mathbf{D} + \frac{\eta_{po}}{\tau_d}\langle R^2\rangle\,\langle\mathbf{uu}\rangle\,,$$

$$\frac{D\langle\mathbf{uu}\rangle}{Dt} = \nabla\mathbf{v}\cdot\langle\mathbf{uu}\rangle + \langle\mathbf{uu}\rangle\cdot\nabla\mathbf{v}^T - 2\nabla\mathbf{v}:\langle\mathbf{uu}\rangle\,\langle\mathbf{uu}\rangle - \frac{1}{\tau_d\langle R^2\rangle}\left(\langle\mathbf{uu}\rangle - \frac{1}{3}\mathbf{I}\right),$$

$$\frac{D\langle R^2\rangle}{Dt} = 2\,\langle R^2\rangle\,\nabla\mathbf{v}:\langle\mathbf{uu}\rangle - \frac{1}{\tau_R}(\langle R^2\rangle - 1)\,.$$

2. Analytical Solution for Model A. In Cartesian coordinates, the one-dimensional ($v_x(y)$ and $v_y = v_z = 0$) steady-state flow in a long plane channel is described by the equation

$$\frac{\partial\tau_{xx}}{\partial x} + \frac{\partial\tau_{xy}}{\partial y} = \frac{\partial p}{\partial x}\,. \tag{1}$$

When the viscosity coefficient μ is constant, all the components of the extra-stress tensor are independent of x while all the derivatives with respect to x except dp/dx = const are equal to zero, and Eq. (1) can be integrated once. Taking account of the fact that $\tau_{xy} = 0$ at $y = 0$, we obtain

$$\tau_{xy} = \frac{dp}{dx}y\,. \tag{2}$$

The components of the extra-stress tensor in plane-parallel flow are determined by the following expressions:

$$\tau_{xx} + \tau_{xy}\lambda_1\left(\frac{dv_x}{dy}\right)(-1+a+b) = \mu\lambda_2\left(\frac{dv_x}{dy}\right)^2(-1+a+b)\,, \tag{3}$$

$$\tau_{yy} + \tau_{xy}\lambda_1\left(\frac{dv_x}{dy}\right)(1+a+b) = \mu\lambda_2\left(\frac{dv_x}{dy}\right)^2(1+a+b)\,, \tag{4}$$

$$\tau_{zz} + \tau_{xy}\lambda_1\left(\frac{dv_x}{dy}\right)b = \mu\lambda_2\left(\frac{dv_x}{dy}\right)^2 b\,, \tag{5}$$

$$\tau_{xy} + \frac{1}{2}\lambda_1\left(\frac{dv_x}{dy}\right)[(\tau_{xx}-\tau_{yy}) + (\tau_{xx}+\tau_{yy})(a+c)] = \mu\left(\frac{dv_x}{dy}\right). \tag{6}$$

Substituting (3)–(5) into (6) and then into (2), we find

$$\tau_{xy} = \mu\left(\frac{dv_x}{dy}\right)\frac{1+\lambda_1\lambda_2[1-(a+b)(a+c)]\left(\frac{dv_x}{dy}\right)^2}{1+\lambda_1^2[1-(a+b)(a+c)]\left(\frac{dv_x}{dy}\right)^2} = \frac{dp}{dx}y\,. \tag{7}$$

For the flow with a prescribed gradient we must determine the rate of shear and the velocity profile from the solution of the equation of motion (7). We will assume that $(a+b)(a+c) \neq 1$. Otherwise we obtain a trivial solution with a parabolic velocity profile.

After the introduction of the dimensionless parameters $\xi = y/h$, $\varepsilon = \lambda_2/\lambda_1$, and $\alpha = \sqrt{1+(a+b)(a+c)}$ and the dimensionless longitudinal velocity $V = v_x\lambda_1\alpha/h$, rate of shear $q = \lambda_1\alpha dv_x/dy$, and pressure gradient $G = -2\Delta p\lambda_1\alpha h/\mu L$, we have

$$2q\frac{1+\varepsilon q^2}{1+q^2} = -G\xi\,. \tag{8}$$

For the prescribed pressure gradient, Eq. (8) describes the distribution of the dimensionless rate of shear as a function of the dimensionless coordinate ξ. It is nonlinear and can have several solutions for q.

To compute the velocity profile we must take the following integral:

$$V = \int q\,d\xi + C = \int q\frac{d\xi}{dq}\,dq + C\,. \tag{9}$$

We can compute the derivative $\frac{d\xi}{dq} = \frac{2}{G}\frac{(1-q^2+3\varepsilon q^2+\varepsilon q^4)}{(1+q^2)^2}$ from (8) and, using (9), find the longitudinal velocity as a function of the rate of shear:

$$V = \left\{\varepsilon(1+q^2) + (\varepsilon-1)\left[\ln|1+q^2| + \frac{2}{1+q^2}\right] + C\right\}\frac{1}{G}\,. \tag{10}$$

The integration constant C is determined from the boundary conditions $V = 0$ and $q = q_w$ at $\xi = \pm 1$:

$$C = -\varepsilon(1+q_w^2) - (\varepsilon-1)\left[\ln|1+q_w^2| + \frac{2}{1+q_w^2}\right].$$

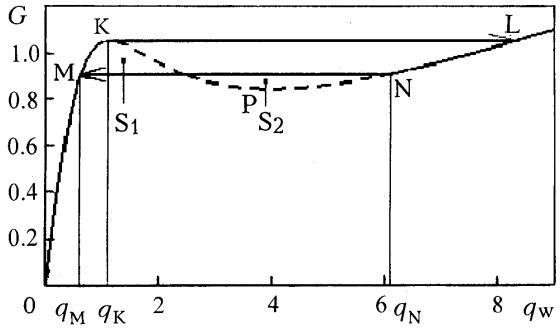

Fig. 1. Dimensionless pressure drop G vs. dimensionless rate of shear on the channel wall q_w for $\varepsilon = 0.05$.

On the other hand, the transverse coordinate ξ can also be written from Eq. (8) as a function of q:

$$\xi = -\frac{2q\,(1+\varepsilon q^2)}{1+q^2}\,\frac{1}{G}. \tag{11}$$

Finally, the profile of the longitudinal velocity can be represented in parametric form:

$$V = \frac{(1+q_w^2)\left[\varepsilon\,(q_w^2-q^2)+(1-\varepsilon)\left(\ln\left|\frac{1+q^2}{1+q_w^2}\right|+\frac{2\,(q_w^2-q^2)}{(1+q^2)\,(1+q_w^2)}\right)\right]}{2q_w\,(1+\varepsilon q_w^2)}, \quad \xi = \frac{q\,(1+\varepsilon q^2)\,(1+q_w^2)}{q_w\,(1+q^2)\,(1+\varepsilon q_w^2)}, \tag{12}$$

where the rate of shear on the wall q_w is related to the pressure gradient G by the relation

$$2q_w\,\frac{1+\varepsilon q_w^2}{1+q_w^2} = -G. \tag{13}$$

The prescribed value of the pressure gradient G, when $\varepsilon < 1/9$, can correspond to one, two, or three values of the rate of shear on the wall q_w.

Let us consider by way of example the dimensionless pressure gradient G as a function of the parameter q_w plotted according to Eq. (13) at $\varepsilon = 0.05$ (Fig. 1). Flow is physically unrealizable on the descending portion of the G–q_w curve between points K and P and on the ascending portion between points P and N. Thus, motions corresponding to the ascending portions of the G–q_w curve from 0 to point K and from point N and higher can be observed in nature. In Fig. 1, the portions of the curve that correspond to physically feasible linearly stable regimes are shown solid, while the portions of the curve that correspond to unrealizable regimes are shown dashed.

We will assume that flow occurs in the regime of a prescribed pressure gradient G. As it smoothly increases, we have subcritical bifurcation, i.e., nonuniqueness of the solution appears before the critical value of the pressure gradient G_{max} is attained. Since branching subcritical solutions are unstable at infinitely small disturbance amplitudes, one cannot observe continuous bifurcation in nature. Instead, we have a discontinuous process in which the disturbed solution, leaving the domain of attraction of the solution corresponding to the main flow, will pass through the unstable branching solution to a stable solution with a much-higher-than-average velocity. The velocity profiles of the polymer solution for this new linearly stable regime necessarily have closed loops, which leads to weak tangential discontinuities (the function is continuous, the jump is in the derivative) or strong tangential discontinuities (the jump is in the function itself). The latter are unstable to infinitely small disturbances now. Therefore, only weak tangential discontinuities can be realized, which correspond to the passage along the line $\overline{MN}$ arranged so that the areas of the domains S_1 and S_2 (see Fig. 1) are equal. Figure 2 gives the velocity profiles in the case of a jump from point K to point L;

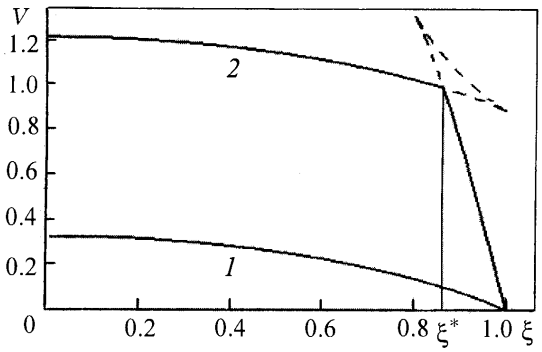

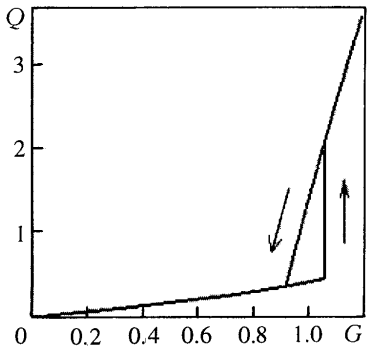

Fig. 2. Velocity profiles for $G = G_{max} = 1.0559$ and $\varepsilon = 0.05$: 1) velocity at point K and 2) at point L.

Fig. 3. Hysteresis of the head-flow-rate characteristics for $\varepsilon = 0.05$.

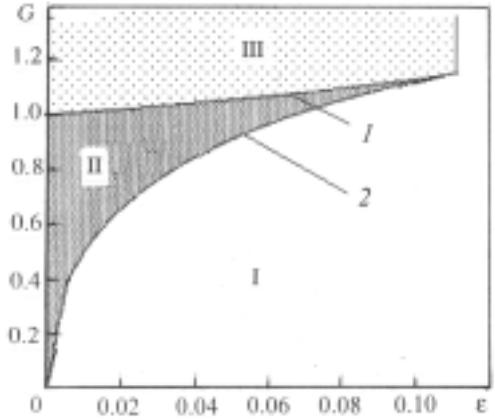

Fig. 4. Phase plane G–ε [1) G_{max}; 2) G_{eq}]: I, stability domain (the solution is unique, the velocity profile is smooth and nearly parabolic); II, metastability domain (two solutions stable to infinitely small disturbances and unstable in relation to disturbances of finite amplitude); III, stability domain (the solution is unique, the velocity profile has weak tangential discontinuities).

they have been constructed according to formulas (12) at the same pressure gradient G_{max}, which is critical for this ε. The dashed line denotes the unrealizable loops corresponding to the passage along the $\overline{MN}$ line.

As the pressure gradient smoothly decreases, reverse passage to the left-hand branch of the curve is along the $\overline{MN}$ line (Fig. 1) at $G_{eq} < G_{max}$. At this value of G, the branch point of the second solution turns out to be at the channel boundary, while inside the channel the velocities are totally coincident with the first solution. Thus, there is no variation of the velocity in the case of a smooth decrease in the pressure gradient.

From the velocity profile found we can compute the dimensionless flow rate Q of the polymer solution moving in the channel by integrating the velocity profile over the channel depth. For the values $\varepsilon \geq 1/9$ the integrand is smooth and a certain integral is taken over the entire depth of the channel:

$$Q = 2\int_0^1 V d\xi = 2\int_0^{q_w} V \frac{d\xi}{dq}\, dq\,. \tag{14}$$

For $\varepsilon < 1/9$, in active loading $dG > 0$ and $G > G_{max}$ and in unloading $dG < 0$ and $G > G_{ef}$, the integrand has a closed loop with a branch point inside the channel, and to compute the flow rate we must subdivide the evaluated integral into the sum of two integrals with the limits from 0 to q_M and from q_N to q_w in which the integrand is monotonic:

$$Q = 2\int_0^{\xi^*} V d\xi + 2\int_{\xi^*}^{1} V d\xi = 2\int_0^{q_M} V\frac{d\xi}{dq}\,dq + 2\int_{q_N}^{q_w} V\frac{d\xi}{dq}\,dq\,. \tag{15}$$

One can also determine the dependence of the flow rate on the dimensionless pressure gradient in parametric form by adding relation (13) to Eq. (14) or (15).

From the fact that, as G increases and drops, passages from one branch of the curve to the other occur at different critical values of G, the head-flow-rate characteristic has a hysteresis (Fig. 3). The arrows in the figure indicate the direction followed by the process with increase or decrease in the pressure gradient.

For the values $\varepsilon < 1/9$ there is a certain interval G_{eq}–G_{max} in which the main motion is metastable, i.e., stable in relation to infinitely small disturbances and unstable in relation to disturbances of finite amplitude. Critical for this type of flow is the empirical condition $G_{max} = 1 + 0.2376\varepsilon$. In particular, for the De Witt model this is $G_{max} = 1$. In the subcritical regime $G_{max} \le 1$, the velocity profiles are continuously smooth and nearly parabolic. In the supercritical regime $G_{max} > 1$ and at $(a + b)(a + c) < 1$, the velocity profiles have weak tangential discontinuities in the general case, while for Maxwell-type models ($\lambda_2 = 0$) there exist no kinematically feasible solutions of any sort.

In the phase plane G–ε (Fig. 4), we can separate the domain where the problem has a unique stable solution (domain I) and the domain of metastable stability — the solution is stable in relation to infinitely small disturbances and unstable in relation to disturbances of finite amplitude (domain II). Here one linearly stable solution is realized depending on the loading prehistory. A unique stable solution with weak tangential discontinuities is realized in domain III.

3. Analytical Solution for Model B. In the case of the stationary plane-parallel flow ($v_x = v_x(y)$, $v_y = 0$, and $v_z = 0$) for the five unknowns v_x, $u = \langle \mathbf{uu} \rangle_{xy}$, $v = \langle \mathbf{uu} \rangle_{xx}$, $w = \langle \mathbf{uu} \rangle_{yy}$, and $r = \langle R^2 \rangle$ we have five differential equations

$$\frac{1}{1+k}\frac{d}{d\xi}\left(\frac{dV}{d\xi}\right) + \frac{k}{1+k}\frac{d(ur)}{d\xi} = -G\,, \tag{16}$$

$$\left(u^2 - \frac{w}{2}\right)\frac{dV}{d\xi} + \frac{u}{r} = 0\,, \tag{17}$$

$$(v-1)\,u\frac{dV}{d\xi} + \frac{v - \frac{1}{3}}{r} = 0\,, \tag{18}$$

$$uw\frac{dV}{d\xi} + \frac{w - \frac{1}{3}}{r} = 0\,, \tag{19}$$

$$ur\frac{dV}{d\xi} - \frac{r-1}{\varepsilon} = 0\,, \tag{20}$$

where $\xi = y/h$, $k = \eta_{po}/\eta_s$, $V = v_x\tau_d/h$, $\varepsilon = \tau_R/\tau_d$, $G = -\Delta p\tau_d h/L\eta_0$, and $\eta_0 = \eta_s + \eta_{po}$, and the boundary conditions of sticking for the velocity: $V = 0$ at $\xi = \pm 1$.

Equation (16) can be integrated once. Introducing the dimensionless rate of shear $q = \tau_d dv_x/dy$, with allowance for the fact that $q = 0$ and $u = 0$ at $\xi = 0$, we obtain

$$\frac{q}{1+k} + \frac{kur}{1+k} = -G\xi\,. \tag{21}$$

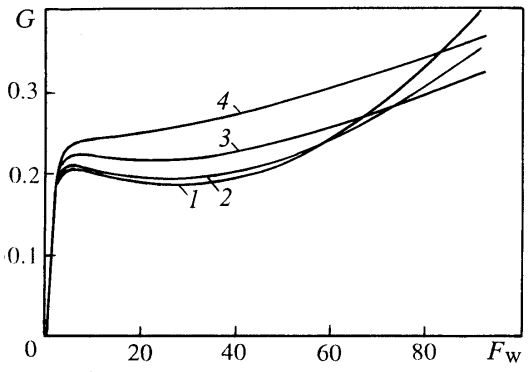

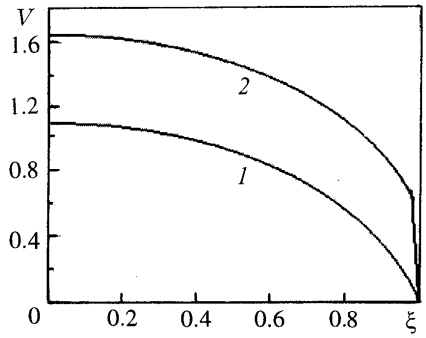

Fig. 5. Dimensionless pressure drop vs. parameter F_w for k = 1000: 1) ε = 0, 2) 0.01; 3) 0.05, and 4) 0.1.

Fig. 6. Two velocity profiles existing at the same critical pressure drop G_{max} = 0.22176, k = 1000, and ε = 0.05: 1) subcritical regime; 2) supercritical regime.

We introduce the parameter $F = (r-1)/\varepsilon$ and solve system (17)–(21) relative to the parameter F. From solution of the system of equations (18) and (20) we have

$$u = \frac{F}{qr}, \tag{22}$$

$$v = \frac{3F+1}{3(F+1)} \tag{23}$$

and from the system of equations (17) and (19), with account for (22) and (23), we obtain

$$r = \frac{\sqrt{6}\sqrt{F}(F+1)}{q}, \tag{24}$$

$$w = \frac{1}{3(F+1)}. \tag{25}$$

The rate of shear q can also be expressed from (24) by the parameter F:

$$q = \frac{\sqrt{6}\sqrt{F}(1+F)}{1+\varepsilon F}. \tag{26}$$

To find the velocity profile we must take the following integral:

$$V = \int dq\xi + C = \int q\frac{d\xi}{dF}dF + C. \tag{27}$$

Then we can compute the derivative $d\xi/dF$ from (21) and, taking the integral in (27), express the longitudinal velocity V and the dimensionless coordinate ξ by the parameter F:

$$V = \frac{1}{G(1+k)}\left\{k\ln\left|\frac{1+F}{(1+\varepsilon F)^{1/\varepsilon}}\right| + \frac{kF}{2} + \frac{3F}{\varepsilon^2} + \frac{3(\varepsilon^2-4\varepsilon+3)}{\varepsilon^3(1+\varepsilon F)} - \frac{3}{\varepsilon^3}\frac{(\varepsilon^2-2\varepsilon+1)}{(1+\varepsilon F)^2}\right\} + C,$$

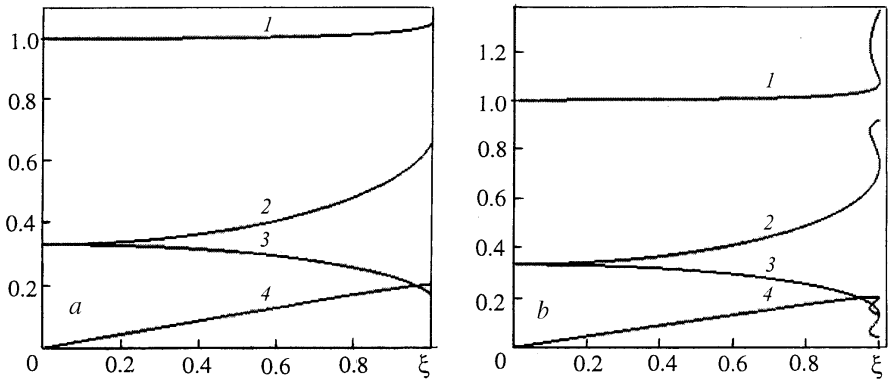

Fig. 7. Profiles of the elongation [1] $r = \langle R^2 \rangle$] and of the orientation-tensor components [2] $v = \langle \mathbf{uu} \rangle_{xx}$, 3) $w = \langle \mathbf{uu} \rangle_{yy}$, 4) $u = \langle \mathbf{uu} \rangle_{xy}$]: a) subcritical regime; b) supercritical regime.

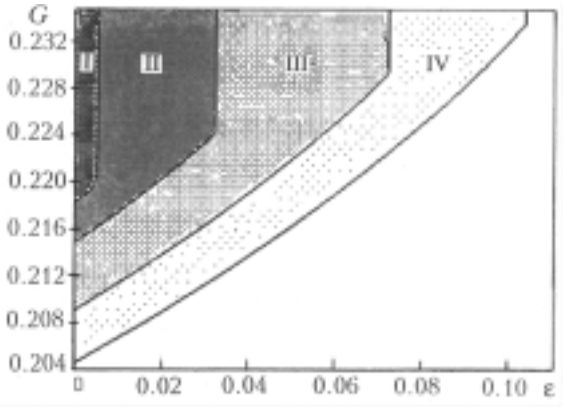

Fig. 8. Regions of the critical values of the pressure gradient for different k: I) k = 400, II) 500, III) 1000, and IV) 10,000.

$$\xi = -\frac{1}{G}\frac{\sqrt{6}\,\sqrt{F}}{(1+k)}\left[\frac{k\,(1+\varepsilon F)^2 + 6\,(1+F)^2}{6\,(1+F)\,(1+\varepsilon F)}\right]. \tag{28}$$

The integration constant C is determined from the boundary condition $V = 0$ and $F = F_w$ at $\xi = \pm 1$.

The dimensionless pressure gradient G and the parameter F_w are related by the expression

$$\frac{\sqrt{6}\,\sqrt{F_w}}{(1+k)}\left[\frac{k\,(1+\varepsilon F_w)^2 + 6\,(1+F_w)^2}{6\,(1+F_w)\,(1+\varepsilon F_w)}\right] = -G\,. \tag{29}$$

Figure 5 gives the dimensionless pressure gradients G as functions of the parameter F_w at k = 1000 for different ε.

At the prescribed pressure gradient G and when $\varepsilon < 1/9$, there can exist one, two, or three values of the parameter F_w. The velocity profiles for two solutions existing at the same pressure gradient $G = G_{max}$ are given in Fig. 6. It is obvious that models A and B yield analogous dependences of the dimensionless pressure gradient on the corresponding parameters and similar profiles of longitudinal velocities. Therefore, all the arguments concerning the existence and stability of solutions and given in Sec. 2 are also true of the solutions obtained for model B. However, model B provides additional information on the distribution of the microstructure configuration.

Let us consider, by way of example, the profiles of the elongation r and the distributions of the components of the orientational tensor u, v, and w over the channel height at $G = G_{max} = 0.22176$, k = 100, and ε = 0.05 in subcritical and supercritical regimes. In the first regime, the elongation r smoothly increases from the axis to the channel wall and the statistical-mean orientation also smoothly changes from the isotropic state on the axis to the predominant

orientation along the flow (Fig. 7a). In the second regime, these parameters, smoothly changing almost throughout the interior of the channel, experience a jump near the wall (Fig. 7b).

In model B, just as in model A, critical regimes can occur only when $\varepsilon < 1/9$. This is a necessary but not sufficient condition for model B. For each prescribed value of $0 < \varepsilon < 1/9$ and k there is a limit value of the pressure gradient ($G_{\max}$) the excess over which leads to nonuniqueness of the solution and to tangential discontinuities in the velocity profiles and in the distributions of the elongation and the components of the orientation tensor. For prescribed k and ε the critical values of the pressure gradient are determined from the condition $dG/dF = 0$ and they can be represented in the form of the system relative to $G_{\max}$ and F:

$$G_{\max} = \frac{\sqrt{6}\,\sqrt{F}}{(1+k)}\left[\frac{k\,(1+\varepsilon F)^2 + 6\,(1+F)^2}{6\,(1+F)\,(1+\varepsilon F)}\right], \quad k = -\,6\,\frac{(1+F)^2\,[\varepsilon F\,(F-1) + 3F - 1]}{(1+\varepsilon F)^2\,[\varepsilon F\,(F+3) - F + 1]}. \tag{30}$$

The solution of system (30) is presented graphically in Fig. 8.

For each of the prescribed values of the parameter k the regions lying lower and more to the right of the corresponding curves belong to the subcritical values of the dimensionless pressure gradient, the regions lying higher and more to the left belong to the supercritical regimes in which the problem has a nonunique solution, and the profiles of the velocity, the elongation, and the orientation-tensor components have tangential discontinuities.

This work was carried out with support form the Russian Foundation for Basic Research, project code 01-01-96485.

NOTATION

I, unit tensor; ·, scalar product; :, double scalar product; tr(·), trace of the tensor; $\langle\cdot\rangle$, statistical averaging; x, y, z, Cartesian coordinates, m; ∇, Hamiltonian, m^{-1}; $2h$, channel depth, m; ρ, density, kg/m^3; **v**, velocity vector, m/sec; p, pressure, Pa; τ, extra-stress tensor, Pa; $\nabla\mathbf{v} = \mathbf{D} + \mathbf{W}$, velocity gradient, sec^{-1}; $\mathbf{D} = (\nabla\mathbf{v}^T + \nabla\mathbf{v})/2$, symmetric part of $\nabla\mathbf{v}$, deformation-rate tensor, sec^{-1}; $\mathbf{W} = (\nabla\mathbf{v}^T + \nabla\mathbf{v})/2$, antisymmetric part of $\nabla\mathbf{v}$, vorticity tensor, sec^{-1}; μ, coefficient of viscosity, Pa·sec; λ_1 and λ_2, times of relaxation and retardation, sec; F_{abc}, objective time derivative, sec^{-1}; a, b, and c, dimensionless material constants; D/Dt, substantial time derivative, sec^{-1}; C, integration constant; $k = \eta_{po}/\eta_s$, dimensionless parameter of concentration; η_{po}, polymer viscosity, Pa·sec; η_s, solvent viscosity, Pa·sec; τ_d, orientational relaxation time, sec; τ_R, relaxation time of elongation (according to Rouse), sec; **R**, dimensionless vector describing the elongation and orientation of the chain; R, equilibrium-length-scaled dimensionless distance between the ends of the chain; **u**, unit vector in the direction of elongation of the chain; $G_{\max}$, dimensionless critical pressure gradient; G_{eq}, dimensionless equivalent pressure gradient; Q, dimensionless flow rate of the polymer. Superscripts: T, transposition of the tensor; *, value of the quantity at the branch point. Subscripts: x, y, z, Cartesian components of the vector; xx, yy, zz, and xy, Cartesian components of the tensor; d, orientational relaxation time (disengagement); w, wall; max, maximum value; eq, equivalent value; s, solvent; po, polymer.

REFERENCES

1. T. Mcleish and R. Ball, *Polym. Phys. B, Polym. Phys.*, **24**, 1735–1745 (1986).
2. D. S. Malkus, J. A. Nohel, and B. J. Plohr, *J. Comput. Phys.*, **87**, 464–487 (1990).
3. D. Vlassopoulos and S. G. Hatzikiriakos, *J. Non-Newtonian Fluid Mech.*, **57**, 119–136 (1995).
4. P. Callaghan, M. Cates, C. Rofe, and J. Smeulders, *Journal de Physique II*, **6**, 375–393 (1996).
5. C. F. J. Den Doelder, R. J. Koopmans, J. Molenaar, and A. A. F. Van De Ven, *J. Non-Newtonian Fluid Mech.*, **75**, 25–41 (1998).
6. M. Doi and S. F. Edwards, *The Theory of Polymer Solution*, Oxford (1986).
7. G. Marrucci and N. Grizzuti, *Gaz. Chim. Ital.*, **118**, 179–185 (1988).
8. J. Remmelgas, G. Harrison, and G. Leal, *J. Non-Newtonian Fluid Mech.*, **80**, 115–134 (1999).
9. J. Remmelgas and G. Leal, *J. Non-Newtonian Fluid Mech.*, **90**, 187–216 (2000).